JOURNAL OF AGRICULTURAL AND FOOD CHEMISTRY

Proteomics Analysis of Rat Brain Protein Modulations by Grape Seed Extract

JESSY DESHANE,[†,‡] LISA CHAVES,[‡] KIRAN VARMA SARIKONDA,[†] SCOTT ISBELL,[§] LANDON WILSON,[§] MARION KIRK,[§] CLINTON GRUBBS,[#,Δ] STEPHEN BARNES,[†,‡,§,⊥,Δ] SREELATHA MELETH,[Δ,○] AND HELEN KIM*[,†,‡,§,⊥,Δ]

Department of Pharmacology and Toxicology, Department of Surgery, Biostatistics Unit, and Mass Spectrometry Shared Facility, University of Alabama at Birmingham Comprehensive Cancer Center, Birmingham, Alabama 35294; 2D Proteomics Laboratory, Purdue University−UAB Botanicals Center for Age-Related Diseases, and UAB Center for Nutrient−Gene Interaction in Cancer Prevention, University of Alabama at Birmingham, Birmingham, Alabama 35294

Dietary supplements such as grape seed extract (GSE) enriched in proanthocyanidins (PA) (oligomeric polyphenols) have been suggested to have multiple health benefits, due to antioxidant and other beneficial activities of the PA. However, a systematic analysis of the molecular basis of these benefits has not been demonstrated. Because the brain is vulnerable to age-related oxidative damage and other insults including inflammation, it was hypothesized that rats ingesting GSE would experience changes in expression or modifications of specific brain proteins that might protect against pathologic events. Normal adult female rats were fed diets supplemented with 5% GSE for 6 weeks. Proteomics analysis (2D electrophoresis and mass spectrometry) of brain homogenates from these animals identified 13 proteins that were altered in amount and/or charge. Because many of these changes were quantitatively in the opposite direction from previous findings for the same proteins in either Alzheimer disease or mouse models of neurodegeneration, the data suggest that these identified proteins may mediate the neuroprotective actions of GSE. This is the first identification and quantitation of specific proteins in mammalian tissues modulated by a dietary supplement, as well as the first to demonstrate links of such proteins with any disease.

KEYWORDS: Grape polyphenols; dietary supplement; 2D electrophoresis; mass spectrometry; dementia

INTRODUCTION

Americans currently spend billions of dollars on over-the-counter dietary supplements such as *Ginkgo biloba*, cranberry, St. John's wort, soy isoflavones, and grape seed extract (GSE) (*1*). Several of these, including GSE, are thought to have health benefits due to their high content of polyphenolic compounds, which have been shown to have antioxidant activity in vitro (*2*). GSE in particular is enriched in the proanthocyanidins (PA), oligomeric polyphenols whose precursors, the anthocyanins, account for the deep coloration of many fruits and vegetables, particularly berries. In fruits, PA (the basic structure of which is shown in **Figure 1**) may protect the plants from photo-oxidation due to their general aromatic structure. Previous experiments suggested that antioxidant activity intrinsic to PA such as in GSE may have cardioprotective (*2*−*4*) as well as anticancer properties (*5*). Moreover, recent studies showed that dietary supplementation with aqueous fruit or vegetable extracts high in PA (strawberry, spinach, blueberry) protected rats against age-related cognitive impairment, suggesting that fruit/vegetable-derived PA have neuroprotective activity (*6*). However, *G. biloba* extract, which contains polyphenols different from the fruit PA, has also been shown to protect against β-amyloid-induced oxidative stress in neurons (*7*, *8*). Thus, a variety of supplements and foods enriched in polyphenols appear to have health benefits, but the molecular basis of these actions in target tissues has only begun to be examined. We hypothesized that the actions of dietary supplements such as GSE enriched in PA would be correlated with changes in the target tissues in specific proteins either in their expression or in their post-translational modifications. We utilized proteomics technology to assess the effects of GSE on proteins in the brains of normal rats that had ingested a defined diet supplemented with 5% GSE over a 6-week period. This time period is a widely used time interval during which potential toxicity of drugs or chemical treatments is assessed in rats. Aside from our initial observation that soy

* Address correspondence to this author at the Department of Pharmacology and Toxicology, University of Alabama at Birmingham, McCallum Building, Rm 460, 1918 University Blvd., Birmingham, AL 35294 [e-mail helenkim@uab.edu; telephone (205) 934-3880; fax (205) 934-6944].
[†] Department of Pharmacology and Toxicology.
[‡] Purdue Univeristy-UAB Botanicals Center for Age-Related Diseases.
[§] Mass Spectrometry Shared Facility.
[#] Department of Surgery.
[Δ] UAB Center for Nutrient-Gene Interaction in Cancer Prevention.
[⊥] 2D Proteomics Laboratory.
[○] Biostatistics Unit.

10.1021/jf040407d CCC: $27.50
Published on Web 12/07/2004

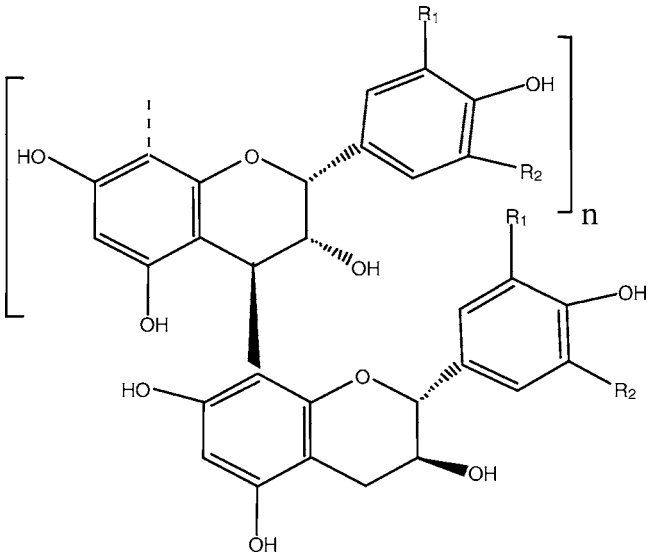

Figure 1. Basic structure of proanthocyanidins. These are polyphenolic compounds enriched in the skins and seeds of many fruits and vegetables, including grapes. The basic subunit, catechin, is indicated in brackets; *n* (the number of catechin monomeric subunits) can be as high as 10. Depending on the proanthocyanidin, R_1 and R_2 can be H or OH.

isoflavones attenuated Alzheimer's disease (AD)-relevant microtubule-associated protein τ phosphorylations in a primate model of menopause (*9*, *10*), there has been little molecular analysis of protein targets of dietary supplements or phytochemicals such as PA in mammalian tissues.

MATERIALS AND METHODS

Processing Rat Brain Samples for Proteomics Analysis. Normal adult female Sprague−Dawley rats, 35 days old, were segregated into two dietary groups (five per group) and maintained on rodent diet AIN-76A (Teklad Industries, Madison, WI), with one group receiving 5% (g/100 g of total diet) supplementation with a powdered GSE preparation (Kikkoman Corp., Chiba, Japan) (*11*). Over 85% of this preparation consisted of polyphenols, and PA comprised 90% of these polyphenols (Table A of the Supporting Information). At 6 weeks, body weights were recorded and the animals euthanized. Whole brains above the brain stem were dissected out, weighed, snap-frozen in liquid nitrogen, and then stored at −80 °C. No significant differences in body weight gain or final organ weights (brain, heart, liver, and uterus) were detected over the duration of the study, nor was any acute toxicity recorded at necropsy (*60*). All of the experiments in this study were reviewed and approved by the University of Alabama at Birmingham Institutional Animal Care and Use Committee.

Two-Dimensional (2D) Electrophoresis. For 2D electrophoresis, a sagital cut was made at the midline of each frozen brain; the left hemisphere was re-archived at −80 °C, and the other half was weighed and homogenized with a Dounce homogenizer at room temperature at a tissue/buffer ratio of 1 g:5 mL in isoelectric focusing (IEF) lysis buffer [7 mol/L urea, 2 mol/L thiourea, 4% 3-[(3-cholamidopropyl)dimethylammonio]-1-propanesulfonate (CHAPS), 5 mmol/L tributylphosphine (TBP)] adjusted with a tablet of Complete Mini, EDTA-free protease inhibitor cocktail (Roche, Mannheim, Germany) (1 tablet per 10 mL of solution). After centrifugation at 100000*g* for 10 min at room temperature, the supernatant was collected and assayed for protein concentration. An aliquot containing 200 μg of protein was diluted to 200 μL with IEF rehydration buffer [lysis buffer adjusted to 1% ampholytes (IPG buffer, Amersham Biosciences, Piscataway, NJ) and a trace amount of bromophenol blue], and an 11-cm immobilized pH gradient (IPG) strip (Amersham Biosciences) containing a pH 4−7 gradient was rehydrated overnight at room temperature with this sample under mineral oil. IEF was carried out on a Multiphor II flatbed apparatus (Amersham Biosciences) cooled to 18 °C following the manufacturer's instructions; total run time was 6 h, or 3.5 kVh. After IEF, the strips were lightly blotted to drain off excess oil and stored at −80 °C overnight. For the second-dimension electrophoresis, each IPG strip was agitated for 20 min at room temperature in sodium dodecyl sulfate−polyacrylamide gel electrophoresis (SDS-PAGE) equilibration buffer [50 mmol/L Tris-HCl, pH 8.8, 6 mol/L urea, 30% (v/v) glycerol, 2% (w/v) SDS, and trace of bromophenol blue], and laid on top of a 10−20% polyacrylamide gradient Criterion gel (Bio-Rad Laboratories, Hercules, CA). Electrophoresis was carried out at 200 V until the dye reached the bottom of the gel. Triplicate gels were run for each brain homogenate and stained with colloidal Coomassie Gel Code Blue (Pierce Endogen Co., Woburn, MA). Images of the stained gels were acquired with a Bio-Rad GS 710 calibrated imaging densitometer. An additional set of replicate gels was run for the same samples, but stained with the fluorescent dye Sypro Ruby according to the manufacturer's instructions (Molecular Probes, Eugene, OR) to enhance detection of lower abundance proteins. Images of these gels were acquired with an FX ProPlus imager (Bio-Rad). For spot excision from the Sypro Ruby-stained gels, the gels were post-stained with colloidal Coomassie Blue.

2D Western Blots. Affinity-purified goat polyclonal anti-creatine kinase-BB chain antibody (Santa Cruz Biotechnology, Inc., Santa Cruz, CA), mouse monoclonal anti-14-3-3 ϵ antibody (BD Biosciences, San Jose, CA), polyclonal anti-actin antibody (Sigma, St. Louis, MO), and monoclonal mouse anti-heat shock protein-60 antibody (clone 1G1) (Advanced Immunochemical Inc., Long Beach, CA) were used for Western blotting following the manufacturer's recommendations. Goat-anti-rabbit, goat anti-mouse, and rabbit anti-goat peroxidase-conjugated secondary antibodies were purchased from KPL Laboratories (Gaithersburg, MD).

For 2D Western blots, samples were processed through 2D electrophoresis as described above, except that 7-cm IPG strips were used instead of 11-cm strips, and the strips were rehydrated in IEF buffer containing 100 μg of protein. Second-dimension electrophoresis was carried out on mini gels (Bio-Rad), and the proteins were electrotransferred to a polyvinyldifluoride (PVDF) membrane (Immobilon-P, Millipore, Billerica, MA) at 200 mA overnight at 4 °C. The membranes were blocked for 2 h at room temperature in 5% (w/v) nonfat dry milk in Tris-buffered saline containing 0.2% Tween-20 (TBST), followed by overnight incubation at 4 °C in TBST adjusted to 2.5% (w/v) milk containing the appropriate antibody (anti-CK-BB at 1:500, anti-actin at 1:2000, anti-14-3-3- ϵ at 1:1000 and anti-HSP-60 at 1:500). The membranes were then rinsed 3 × 10 min each in TBST followed by incubation for 1 h at room temperature with appropriate secondary antibodies diluted in the same buffer as the primary antibodies. The immunoblots were then washed extensively in TBST (6 × 5 min washes) and visualized using the Lumiglow kit (KPL Laboratories).

Image and Statistical Analysis. A total of 30 2D gel images comprised the initial dataset. These images were processed using PDQuest image analysis software (Bio-Rad). The positions of molecular weight standards that had been electrophoresed adjacent to the acidic end of the IPG strip were used to calibrate the 2D gel *y*-axis for unknown gel spot mass determination. The pH gradient was defined in the horizontal dimension within PDQuest by assuming that the physical ends of the IPG gel bed defined the boundaries of the pH gradient and that the gradient was linear within the strip. For determination of spot intensities and *x*,*y* coordinates, a digitized Gaussian master gel image containing all spots was generated within PDQuest, following matching of protein spots among all gels.

To identify gel spots that differed significantly in intensity or in position between the two groups of gels, datasets including the spot numbers, *x* and *y* coordinates for the spots, and the raw spot intensities were exported out of PDQuest and subjected to statistical analysis using the Statistical Analysis System (SAS v. 09, SAS Institute, Cary, NC). As an initial step, the data were subjected to the Wilcoxon rank sum test (*12*), which determined that the medians of the total protein intensities of the two groups of gels were not significantly different ($p = 0.44$). Individual spot intensities on each gel were normalized to the mean total intensity of its group (GSE or control). The normalized intensities were then divided by the sum of the total intensities of the two groups combined. For a spot to be included in the statistical analysis, it had to meet one of three criteria: (1) it had to be present either in all treatment (GSE) gels or (2) in all control gels or (3) it had

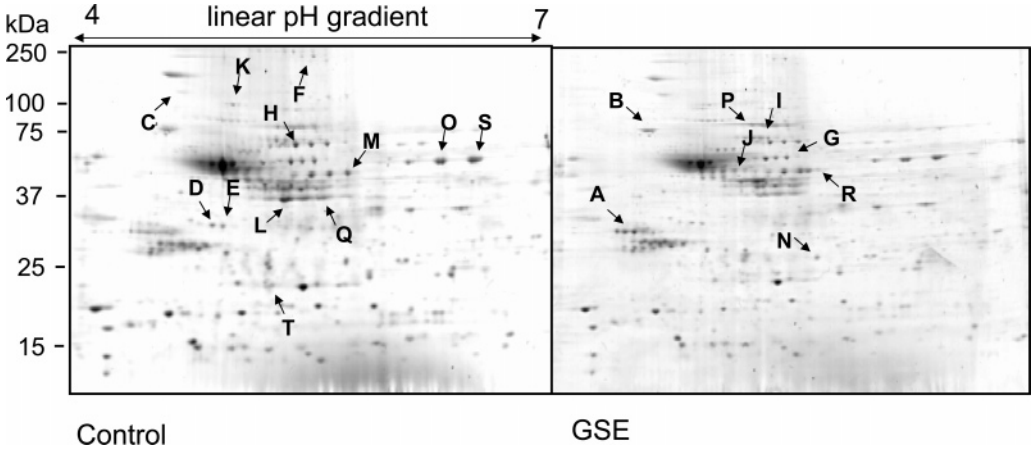

Figure 2. Two-dimensional electrophoretic analysis of rat brain proteins affected by GSE. Brain homogenates from rats exposed dietarily to GSE were electrophoresed on 2D gels incorporating a pH 4–7 gradient in the first dimension and a 10–20% acrylamide gradient in the second dimension. Two hundred micrograms of protein was loaded on all 2D gels in this study. The annotated spots were determined to be significantly different in either intensity or variability between the GSE and control gels, as described in the text. Each spot is indicated once.

to be present in all but one technical replicate of a biological sample. To ensure a normal distribution, spot intensities were log transformed. "Missing" intensities, that is, a gel location containing a spot in one set of gels, but not in the others, were replaced with the lowest log-transformed intensity observed in the experiment, −15.15. Two-sample Student *t* tests and *F* tests were then used to identify spots that differed significantly in intensity or in the variability of the intensity, respectively.

The spots determined to be significantly different in either intensity or variability were then subjected to multivariate analyses such as discriminant analysis (DA) (*13*) and principal component analysis (PCA) (*14*). The spots that were found to be significant on the basis of the two-sample Student *t* test were first run through a stepwise discriminant analysis (SDA) procedure, which compared the spot intensities across the gels and identified the spots that were the best to use in a function that helped to classify the 30 gels correctly into the two groups. These results were then used in DA.

Putative Protein Identifications by Matrix-Assisted Laser Desorption Ionization Time-of-Flight Mass Spectrometry (MALDI-TOF MS). The gel spots of interest indicated by statistical analysis were excised, destained, and subjected to in-gel digestion with trypsin following protocols developed at the National Mass Spectrometry Resource Laboratory at the University of California at San Francisco and described at http://donatello.ucsf.edu/ingel.html. After overnight digestion with trypsin, the tryptic peptides were extracted with 50% acetonitrile/5% formic acid, dried in a Speedvac, and dissolved in 10 μL of 50% acetonitrile/5% formic acid.

The extracted peptides were mixed (1:10, v/v) with a saturated solution of α-cyano-4-hydroxycinnamic acid (Sigma-Aldrich Chemical Co., Milwaukee, WI) in 50% aqueous acetonitrile/0.1% TFA (1:1), and 1 μL of each diluted sample was spotted onto a MALDI-TOF target plate. Peptide mass fingerprint (PMF) analysis was carried out with a Voyager DE-Pro MALDI-TOF mass spectrometer (Perseptive Biosystems, Foster City, CA) according to established procedures in this laboratory (*15*): samples were analyzed in the positive mode with delayed extraction; the acceleration voltage was set at 20 kV; 100 laser shots were summed; bradykinin, angiotensin, and neurotensin were used for external calibration, and the autolysis products of trypsin were used for internal calibration.

The raw MS data for each peptide containing multiple isotope peaks (from the natural abundance of ^{13}C) were processed ("de-isotoped") to identify the $^{1}H/^{12}C$ monoisotopic peak for each peptide, and the resulting peptide masses for a protein were submitted for analysis via the MASCOT search engine (*16*) at http://www.matrixscience.com. The nonredundant NCBI database was used in conjunction with MASCOT to determine putative protein identifications (*17*). The parameters used for searching allowed for all species and one missed trypsin cleavage site. In addition, the mass tolerance for each peptide was set to 100 ppm, that is, 0.1 Da for a peptide with a molecular mass of 1000 Da.

LC-MS/MS. To confirm the putative polypeptide identifications suggested by the MALDI-TOF MS analysis, tryptic digests were analyzed by reverse-phase liquid chromatography−electrospray ionization tandem mass spectrometry (LC-ESI-MS/MS) on a Qtof3 hybrid quadrupole orthogonal time-of-flight mass spectrometer (Waters, Manchester, U.K.). Separation of tryptic peptides by nanoflow liquid chromatography (LC) was accomplished using a FAMOS micro autosampler, a switching device (SWITCHOS), and an Ultimate LC (LC Packings, San Francisco, CA). A sample in 50% acetonitrile/0.1% formic acid was typically diluted 1:1 with water and injected via the autosampler onto a 300 μm i.d. × 5 mm C_{18} μ-precolumn cartridge (LC Packings) at a flow rate of 10 μL/min. After 2 min, elution was accomplished with 80% acetonitrile/0.1% formic acid at 200 nL/s. The resulting eluate was passed into the nanoelectrospray interface of the Q-tof3 mass spectrometer. MS/MS data were recorded using automated MS to MS/MS data-dependent scanning, switching at a threshold of 6 counts. The selected multiply charged ions were subjected to collision-induced dissociation (CID) using argon gas.

RESULTS

Protein Differences between GSE and Control Gels Indicated by Image and Statistical Analysis. Figure 2 shows a typical pair of 2D gels that comprised our dataset. Using criteria described under Materials and Methods, a total of 201 spots were ultimately included in the statistical analysis, from a total of 4500 spots detected among all of the gels. Among these, two types of differences were determined between the gels representing the two dietary groups: differences in *intensity* and differences in *variability* of the intensity. The protein spots that exhibited statistically significant differences in either category are listed in Tables B and C (Supporting Information); a total of 32 spots were determined to be significantly different in intensity between the GSE and control gels (Table B), and 84 spots were significantly different in variability between the two groups of gels (Table C).

DA revealed that of the 32 spots that differed significantly in intensity, only 7 were actually required to discriminate between the two groups with 100% accuracy; of the 84 spots that differed in variability, 25 discriminated between the two groups with 100% accuracy, and, of these, only 8 were required to discriminate between the groups with 93% accuracy. The 7 spots that discriminated 100% due to differences in intensity are indicated in **Figure 2** by letters A−G. These spots, along with spots H−O that also differed significantly in intensity, were selected for analysis by mass spectrometry, and are listed in

Table 1. Gel Spots Significantly Different between GSE and Control Gels

spot ID[a]	fold difference GSE/control[b]	*F* value[c]	*P* value[d]
A*	−1.61		
B*	+1.63		
C	+1.73		
D*	−1.56		
E*	−1.56		
F	−1.6		
G′	−1.61	28.41	<0.0001
H*	+1.5		
I′	+1.63	3.48	0.0261
J	+1.91		
K	−1.52		
L	−1.62		
M′	+1.52	8.17	0.0004
N*	−1.40		
O*	−1.9		
P′		20.22	<0.0001
Q′		6.57	0.0013
R′		3.98	0.0143
S′		3.07	0.0446
T′		4.97	0.0049

[a] Spots were determined via statistical analysis to be significantly different in either intensity or variability between GSE and control gels. The spot ID codes correspond to the annotations in **Figure 2**. Letters with "*****" correspond to the spots that discriminated 100% between the two groups on the basis of intensity; letters with "′" correspond to spots that discriminated 100% between the two groups on the basis of variability, and letters with no other labels are spots which were also significantly different in intensity between GSE and control gels that were excised along with those that discriminated 100% for peptide mass fingerprint analysis. [b] The fold difference (GSE/control) is the difference in intensity of the spot in the GSE gel relative to that in the control gel, after appropriate normalization as described under Materials and Methods. [c] The *F* value is the ratio of the variance of the spot in the GSE gel relative to the variance in the control gel; if there was no difference in variance, the *F* value was 1.00. [d] The *P* value was calculated on the basis of Student's *t* tests.

Table 1. As can be seen, the majority of the significant fold differences in intensity were in the range of 1.5-fold; none were >2-fold. Those spots that discriminated 100% due to differences in variability are also listed in **Table 1** and annotated in **Figure 2** by letters G, I, M, P, Q, R, S, and T. The *F* value shown in **Table 1** is the ratio of the variability in the spot intensity in the GSE gel relative to the variability of that spot in the control gel. (If there were no differences in the variability for a spot, the *F* value would be 1.) Following the statistical analysis, all of the spots in **Table 1** were excised out of appropriate gels for mass spectrometry analysis.

PCA using the spots that discriminated 100% between the two groups of gels confirmed that these spots did indeed cluster the gels according to their groups; **Figure 3A** shows the separation based on differences in intensity, and **Figure 3B** shows the segregation based on differences in variability.

Identification of Proteins That Were Significantly Different in Brains of Rats That Ingested GSE. All of the spots indicated in **Figure 2** that discriminated 100% between the groups of gels, as well as several that were also significantly different in intensity (H−O), were excised, incubated with trypsin, and subjected to peptide mass fingerprint analysis by MALDI-TOF MS, as described under Materials and Methods. **Table 2** lists the putative protein identifications and associated information for each gel spot analyzed by MALDI-TOF MS. It should be noted that ALL of the proteins identified had MOWSE scores above accepted threshold values. Spots N and T (see **Figure 2**) were not included. It should be noted that because the matches obtained by MALDI-TOF MS are matches of one set of peptide masses with another, the identifications are *putative*, and not final (although it is well recognized that MOWSE scores of 70−75 are usually confirmed by sequence analysis by LC-MS/MS). **Table 2** also shows the gene accession number obtained from the analysis within MASCOT, with which one can search protein and gene databases via the search tool Entrez (at http://www.ncbi.nlm.nih.gov) for additional information. It should be noted that once a protein is putatively identified by MALDI-TOF-MS, the predicted mass and isoelectric point (p*I*) that "fall out" from this analysis themselves contribute structural information about the protein, because the observed mass and p*I* (obtained empirically through the image analysis software) are often different from the predicted values. For example, an observed p*I* lower than the predicted p*I* suggests that the protein has undergone post-translational modification such as phosphorylation. Similarly, an observed mass significantly lower than the predicted mass might suggest that the protein undergoes proteolytic processing in vivo. Thus, all of the information from a typical MALDI-TOF MS analysis is valuable, and should be retained, *even in cases when the protein identity itself may not be revealed* (as for spots D and E).

Those protein spots that were significantly *increased* in intensity in the GSE brains were putatively identified as mitochondrial matrix protein precursor P60, also known as heat-shock protein 60 (HSP-60) (**Figure 2**, spot H), heat shock cognate proteins HSC-70 and HSC-71 (**Figure 2**, spots I and J), creatine kinase brain β chain (CK-BB) (**Figure 2**, spots M and R), and neurofilament triplet protein light chain (NF-L) and neurofilament triplet protein medium chain (NF-M) (**Figure 2**, spots B and C). The gel regions containing these spots are shown enlarged in **Figure 4A**. Western blot analysis confirmed the identifications, as well as the quantitative differences in intensities for CK-BB and HSP-60 (**Figure 4B**). Note, however, that in the Western blot analysis, the *total* immunoreactivity for each protein was scanned for densitometric analysis (**Figure 4C**). CK-BB (**Figure 2**, spots M and R) also exhibited a statistically significant difference in isoform complexity (detected as variability) (see **Table 2**), in that the most basic CK-BB isoform was found at a more acidic p*I* in the GSE gels relative to the control gels (**Figure 4A**, right arrow). None of the other spots in the gel region immediately around CK-BB were altered in position in the GSE gel.

Several spots were significantly *lower* in intensity in the GSE gels relative to the control gels. PMF analysis identified these spots as 14-3-3 ϵ protein (**Figure 2**, spot A), actin (**Figure 2**, spot L), glial fibrillary acidic protein (GFAP) (**Figure 2**, spots F and G), vimentin (**Figure 2**, spot K), and α and γ subunits of enolase (**Figure 2**, spots O and P). The gel regions containing these spots are shown enlarged in **Figure 5**. Statistical analysis revealed that 14-3-3 ϵ protein was 1.6-fold lower in intensity in GSE brains relative to control brains, which was confirmed by Western blot analysis (**Figure 5B**,**C**).

Because cytoskeletal components make up a major portion of total protein in neural tissue, it was not surprising that quantitative changes would be found in this category of proteins in this study, although actin has previously been considered to be a "housekeeping" gene; that is, its mRNA level is not changed in response to many stimuli. Following dietary supplementation with GSE, however, the levels of brain actin (**Figure 2**, spots L and Q) were affected, both in level and in isoform complexity; its identification by PMF analysis (**Table 2**) and its lowered expression in GSE gels were confirmed by Western blot analysis (**Figure 5A**,**B**). Other spots that were −1.6- and −1.52-fold lower in intensity in the GSE gels were glial fibrillary acidic protein (GFAP) (**Figure 2**, spot F, MW

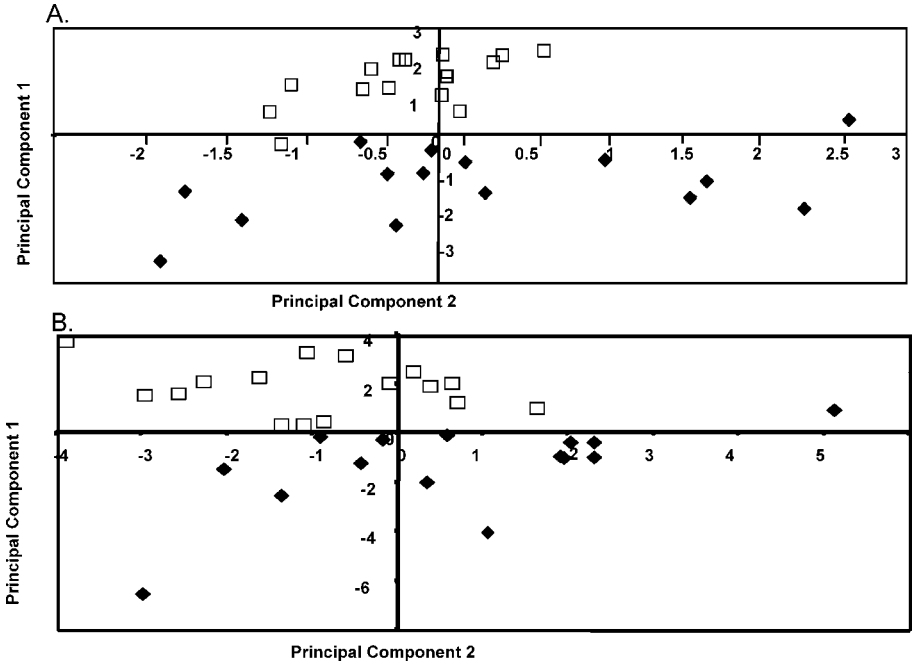

Figure 3. (**A**) PCA of the first and second components of the GSE brains versus the control brains using the significant differences in intensities. (**B**) PCA of the first and second components of the GSE brains versus the control brains, using the significant differences in variability. The open rectangles represent the GSE gels, and the solid diamonds represent the control gels.

250 kDa, and spot G, MW 49 kDa; see also **Figure 5**) and vimentin (**Figure 2**, spot K, and **Figure 5**), respectively. In addition to a lower intensity, the 49 kDa GFAP spot also exhibited a change in variability in the GSE brains that was significantly different between the two sets of gels (see also **Table 2**; **Figure 5**). As **Figure 5** shows, all of the cytoskeletal proteins had multiple gel spots, which were identified by PMF analysis (**Table 2**). It is noteworthy that all of the proteins that were significantly lower in amount between the GSE and control gels were cytoskeletal proteins.

Novel Polypeptides Differentially Expressed in GSE versus Control Brain. Two polypeptides of 26 kDa and p*I* 5.0 had 1.56-fold lower intensity in GSE gels relative to control (**Figure 2**, spots D and E; **Figure 6A**); these two were part of the subset of spots that discriminated 100% between the two groups of gels (**Table 2**). These polypeptides matched with high MOWSE scores (169 for spot D and 95 for spot E) to peptides predicted by a cDNA (NM 025994) in the RIKEN database (*18*); LC-MS/MS analysis confirmed this match (**Figure 6B**). Sequence homology analysis using NCBI BLAST has shown that these polypeptides correspond to a swiprosin-like protein-1, with corresponding accession no. gi34872436. Efforts are underway to characterize these polypeptides and the consequence of changes in their expression following ingestion of GSE.

Although the 2D Western blot analysis confirmed the proteomics identifications and the differences in intensity, we nonetheless carried out conventional one-dimensional SDS-PAGE analysis, in which all 10 brain homogenates in the study were analyzed simultaneously on one gel that was stained for total protein (**Figure 7**). Three replicate gels were Western blotted and probed with the same antibodies against CK-BB, HSP-60, and 14-3-3-ϵ used in the 2D Western blots. As **Figure 7** shows, comparison of the immunoreactivities of equal amounts of total protein for GSE and control brain homogenates gave approximately the same differences in intensity that the statistical analysis and 2D gel Western blots had indicated. It should be noted that for each of the proteins, each immunoreactive band was boxed and quantified as a separate unit, and the average of five determinations for each antigen was then plotted in **Figure 7C**.

Relationship of These Data to Previous Findings. Recent analyses have identified proteomic changes in AD brain after autopsy (*19*, *20*) and in the brains of two mouse models of neurodegeneration, the glycogen synthase kinase-3β (GSK-3β) mouse (*21*) and the Htau40-1 mouse (*22*). We compared the proteins affected by GSE in this study with those that had recently been identified in these previous studies. In the GSK-3β transgenic mouse, overexpression of a constitutively active GSK-3β results in a model of neuropathology similar to AD (*23*). Similarly, the Htau40-1 mouse, which overexpresses the longest isoform of human τ (Htau40-1), results in neurodegeneration similar to that seen in the GSK-3β mouse and in AD (*24*). More proteins were identified to be "different" between pathologic brain and normal or wild type in these papers than in our study; however, it should be noted that Schonberger et al. (*19*) denoted only directions of change, that is, + or −, not quantitative differences. Close comparison of previous results with those in the present study (**Table 3**) showed that wherever there was a common protein, either it was invariably changed by GSE in the opposite direction to what had been found for that protein in the diseased brains or there was a difference in complexity. For example, whereas HSP60 was found at a lower amount in AD brain as well as in the GSK-3β brain, it was increased 1.5-fold in GSE brains relative to the control brains. Similarly, neurofilament L protein (NF-L) was reduced ~2-fold in both mouse models and also was lower in AD; in the brains of animals that ate GSE, however, this protein was increased by 1.63-fold. It should be noted that several proteins detected in the present study as being significantly different in either amount or isoform complexity, actin, RIKEN cDNA NM 025994, and neurofilament M protein (NF-M), were not detectably different in the diseased brain in other studies. In general, however, wherever there was a protein that was identified among any of the three studies and our study, invariably the direction

Table 2. Proteomic Characterization of Polypeptide Differences between GSE and Control Rat Brains[a]

spot ID	protein name	no. of matched peptides	accession no.	MOWSE score	obsd MW (kDa)	predicted MW (kDa)	obsd p*I*	predicted p*I*	peptides sequenced by LC-MS/MS
A	14-3-3 ϵ	10	P42655	1.41E+09*	31.9	29.1	4.5	4.6	
B	neurofilament L triplet protein	14	gi13929098	120	61.0	61.2	4.6	4.6	
C	neurofilament M triplet protein	19	gi8393823	153	95.0	95.6	4.7	4.7	EYQDLLNVK MALDIEIAAYR FSTFSGSITGPLYTHR VQSLQDEVAFLR
D	RIKEN cDNA	9	NP080270	169	26.0	25.1	5.0	5.0	ADLNQGIGEPQSPSR
E	(NM 025994)		NP080270	95	26.0	25.1	5.1	5.0	SMIQEVDEDFDSK
F	GFAP	20	P47819	9.67E+09*	49.0	49.9	5.4	5.3	
G	GFAP	12	P47819	88	230.2	49.9	5.1	5.3	
H	mitochondrial matrix protein precursor P60 (HSP 60)	10	P19227	1.26E+04*	64.9	60.9	5.6	5.9	VGEVIVTKDDAMLLK IQEITEQLDITTSEYEKEK ISSVQSIVPALEIANAHR VGLQVVAVK
I	HSC-70	12	gi4103877	110	70.3	42.5	5.3	6.6	
J	HSC-71	16	gi123644	105	70.3	71.2	5.4	5.4	
K	vimentin	10	gi202368	93	53.6	53.6	5.0	5.0	
L	actin	8	P10365	2.18E+05*	42.0	41.6	5.3	5.4	
M	creatine kinase brain β chain	12	P07335	1.66E+05*	45.6	42.7	5.4	5.3	LEQGQPIDDLMPAQK LLIEMEQR
O	α-enolase	9	P04764	6.64E+05*	46.0	46.9	6.0	6.2	VVGDDLTVTNPK
P	γ-enolase	10	P07323	95	47.0	47.1	5.1	5.0	AAVPSGASTGIYEALELR LDNLMLELDGTENK MVIGMDVAASEFYR
Q	actin	12	gi113307	96	42.1	41.6	5.5	5.4	
R	creatine kinase brain β chain	10	P07335	108	45.6	42.7	5.5	5.3	
S	α-enolase	13	P04764	105	46.0	46.9	6.2	6.2	

[a] The proteins and their associated parameters resulted from PMF analysis carried out by MALDI-TOF MS as described under Materials and Methods. The spot ID refers to the gel spots in **Figure 2** that were excised for the PMF analysis. The number of matched peptides refers to the number of tryptic peptides that were used to identify the protein within MASCOT. The accession number is the identifier assigned to the gene that encodes the polypeptide identified in MASCOT. The MOWSE score is the molecular weight search engine probability score, which indicates the goodness of fit. Asterisks indicate MOWSE scores obtained with PS1 software (Applied Biosystems) that automatically performs the best match for the generated tryptic peptide fingerprint. A PS1 MOWSE score of $>1 \times 10^3$ (1E3) is considered to be statistically significant. A MASCOT MOWSE score of >74 is considered to be statistically significant. Obsd MW and p*I* refer to the empirically determined molecular weight and p*I* for the polypeptide, based on calibration of the 2D gel images within the image analysis software. The predicted MW and p*I* refer to the molecular weight and isoelectric point of the polypeptide predicted by the amino acid sequence encoded by the gene for that polypeptide. The peptides sequenced by LC-MS/MS were obtained as described under Materials and Methods. Note spots D and E, and F and G, were paired, because each pair of spots corresponded to the same polypeptide, as indicated by mass spectrometry.

of change induced by the GSE was in the opposite direction from that detected for the protein by others.

DISCUSSION

In this study, we have shown for the first time that ingestion of a polyphenol-enriched preparation, grape seed extract, resulted in a reproducible set of changes in the amounts and isoform complexities of specific proteins in the brains of normal adult rats. These results were obtained by a combination of 2D electrophoresis, statistical analysis, and mass spectrometry analysis. For several of the proteins, conventional Western blot analysis using commercially available specific antibodies confirmed both identities and differences between GSE and control gels indicated by the statistical and mass spectrometry analysis.

The statistical methods used in this study included the traditional Student *t* tests and *F* tests to initially identify subsets of proteins that were statistically different between the groups. DA then teased out the least number of proteins that could explain the differences between the two treatment groups. Finally, PCA provided a visual representation of the fact that the gels segregate to two groups. These methods have been widely used in the analysis of data from other high-dimensional systems (*29*−*31*).

The high dimensionality (multiple sources of error and variation) of 2D gel analysis introduces many sources of variation that must be controlled for, including protein concentration determination, the passive rehydration of the IPG strips with the protein samples, and instrumentation drift in the imaging step. In view of these various parameters, some variation in total signal from gel to gel was expected and addressed in our study by normalizing the intensity of each spot by the sum of the total spot intensities on the gel. This normalization method is widely used in DNA microarray analysis for similar reasons (*32*). Similarly, normalization was extended across the samples in a group and between treatment groups because nominally the same total amount of protein from all samples from all treatment groups was loaded onto the gel strips. This approach made for a substantially more robust and reliable interpretation of the gel image dataset.

However numerous the options in sophisticated software image analysis packages, a deficiency of most commercial image analysis software, including the one utilized in the present study, is the inability to implement any transformation routines to the data. Biological systems are notorious for data that are not normally distributed (as occurred in the present study). Appropriate transformations (e.g., logarithmic normalization) prior to further statistical analysis were enabled by exporting raw spot intensities into an Excel format followed by log transformation using SAS.

Identification of proteins, whether in gel "spots" or in solution, by peptide mass fingerprinting has become routine. The public availability of search engines such as MASCOT enables any

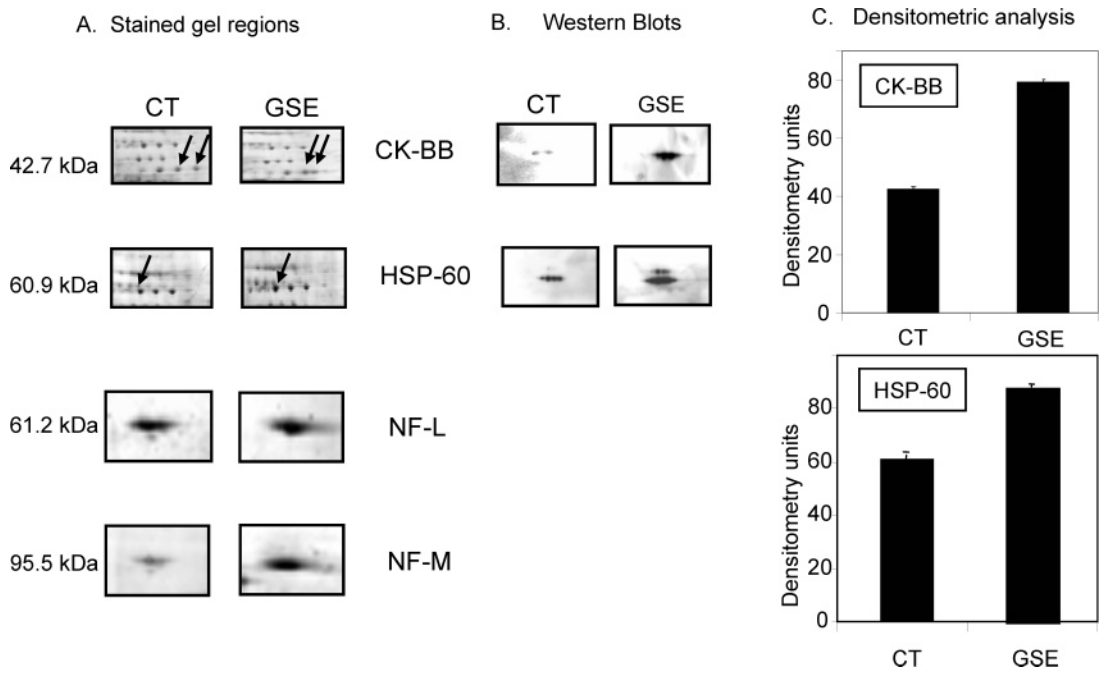

Figure 4. Proteins increased in GSE versus control gels: (**A**) enlarged gel regions showing the spots identified as CK-BB, HSP-60, NF-L, and NF-M by subsequent mass spectrometry; (**B**) 2D Western blots probed with anti-creatine kinase BB chain antibody and anti HSP-60 antibody; (**C**) densitometric analysis of the Western blots shown in panel **B** (mean value ± SE; $n = 3$).

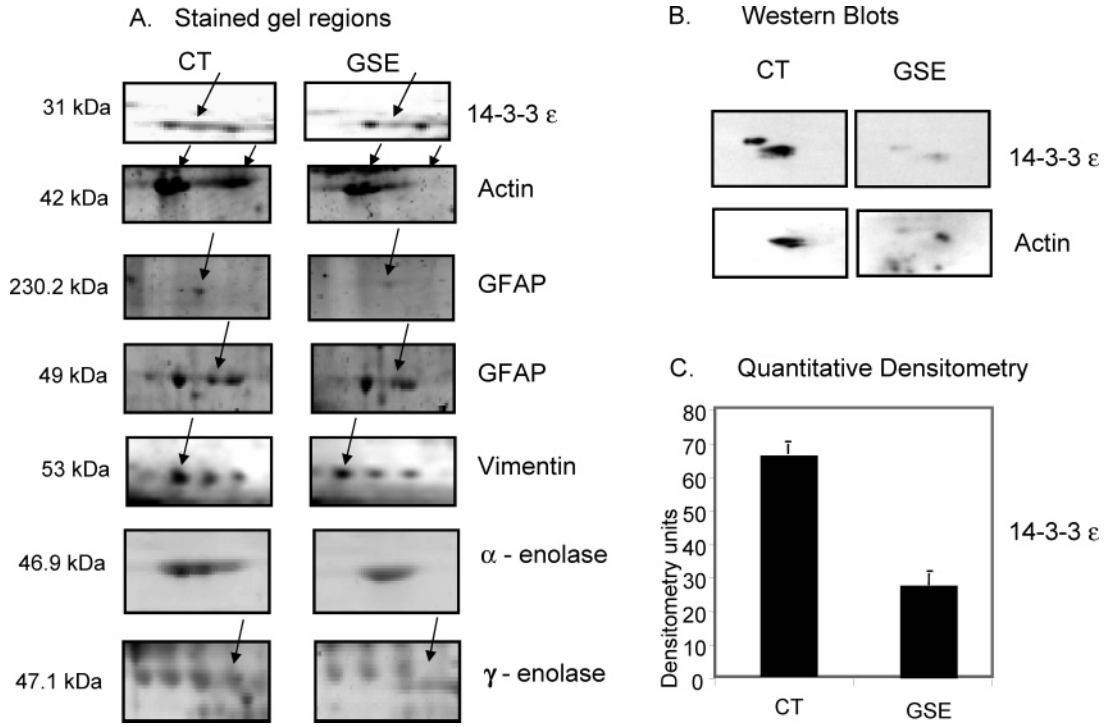

Figure 5. Proteins that were decreased in GSE versus control gels: (**A**) enlarged stained gel regions showing the spots that were subsequently identified as 14-3-3 ϵ protein, actin, GFAP (230 and 49 kDa isoforms, vimentin, and α and γ isoforms of enolase; (**B**) 2D Western blot analysis of 14-3-3 e and actin; (**C**) densitometric analysis of the actin Western blot shown in panel **B** (mean value ± SE; $n = 3$).

investigator with internet access to carry out analysis of proteins of interest. Wise et al. (*33*) previously concluded, at a time when the protein database contained approximately 100 000 entries, that irrespective of the site of cleavage, >90% of proteins could be identified on the basis of two to three peptides with a mass accuracy of 1 Da. Nowadays, typically, identifications are made on the basis of four to eight recognizable peptide masses following trypsin digestion because the large variation in the observed intensities for individual peptides in MALDI-TOF-MS analysis prevents detection of at least 50% of the expected peptides. Because the total number of potential proteins (based on genome sequence information) and observed proteins has substantially increased, several proteins apparently containing the submitted peptides may give rise to similar MOWSE scores. A partial solution is to more accurately determine the mass of each peptide, although this does not always yield conclusive results. A better approach is to carry out tandem mass spectrometry (LC-MS/MS) on the tryptic peptides. In this

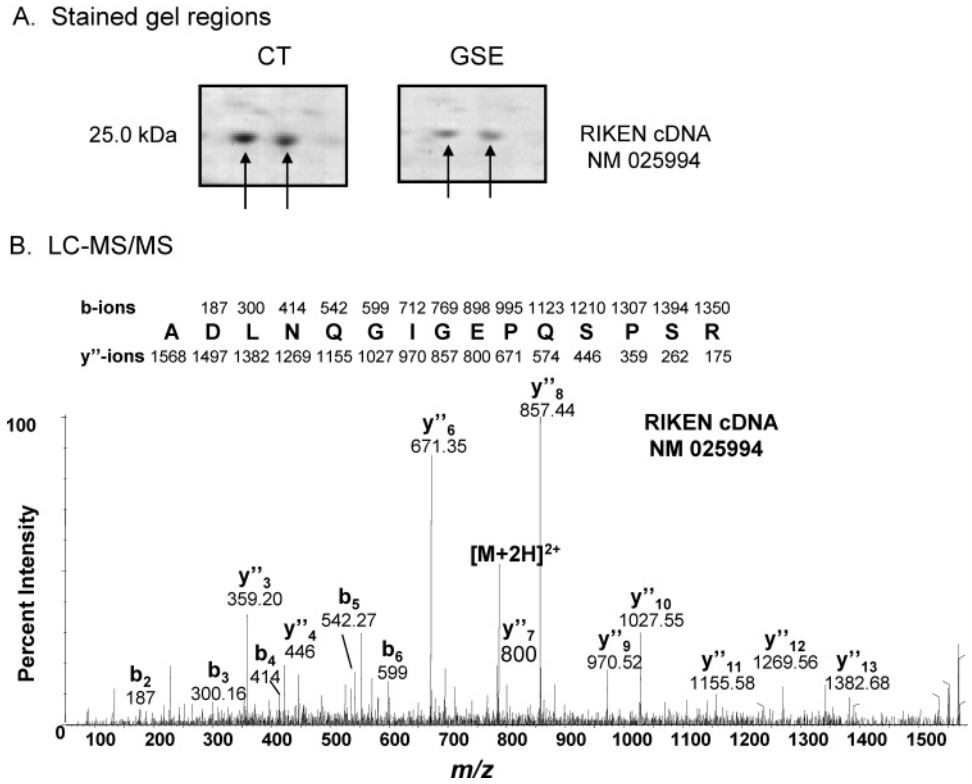

Figure 6. Novel polypeptides lowered in expression in GSE versus control gels: (**A**) enlarged gel regions showing the pair of polypeptide spots at 25 kDa and p*I* 5.0 that differed significantly in intensities between control and GSE gels; (**B**) LC-MS/MS fragmentation pattern that identified these polypeptide spots as highly homologous with the polypeptide encoded by RIKEN cDNA NM 025994. The b and "y" ions that generated the amino acid sequence are indicated above the fragmentation pattern.

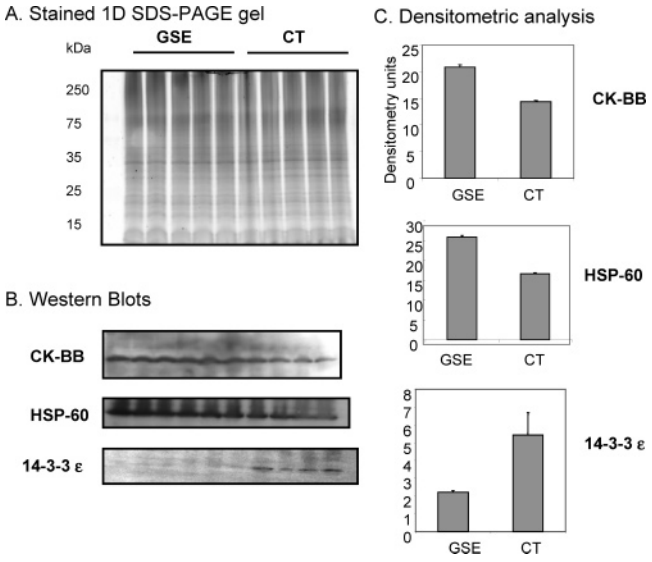

Figure 7. SDS-PAGE Western blot analysis confirms statistical determination of protein expression affected by GSE. Twenty-five micrograms of protein from each of the 10 brain homogenates in this study was electrophoresed on one SDS-PAGE gel. (**A**) One gel was stained with Sypro Ruby, to visualize total proteins. (**B**) Replicate gels as in panel **A** were electrotransferred to PVDF membranes and probed with antibodies against CK-BB, HSP60, and 14-3-3-ϵ. (**C**) Densitometric analysis was performed for the Western blots shown in panel **B**. Each of the 10 lanes in panel **C** was analyzed separately by densitometry; thus, the signal for each protein is an average of five determinations.

technology, CID of the peptides causes fragmentation principally at the peptide bond between residues, producing N-terminal b ions and C-terminal "y" ions (see **Figure 6**). These are predictable, and although not every possible fragment ion is observed in the tandem mass spectrum, a combination of ions is sufficient to identify parts of the internal sequence of the peptide. Therefore, with the confirmed sequence of the peptide, the identity of the protein among the possibilities revealed by peptide mass fingerprinting can usually be made.

Two-dimensional Western blots confirmed the identities of the brain proteins that underwent significant change in response to GSE as well as the quantitative information indicated by the image and statistical analysis. Western blots of 1D SDS-PAGE of all 10 samples electrophoresed on the same gel further confirmed the results.

The statistical analysis used in this study revealed changes in 13 brain proteins that were associated with ingestion of GSE. The proteins that were increased in expression were the heat shock proteins, HSP-60, HSC-70, and HSC-71, which have been suggested to have roles as chaperones in protein folding and assembly and in protein secretion (*34*), as well as in the control of apoptotic pathways (*35*). CK-BB was also increased in amount—this enzyme plays an important role in the brain in regenerating ATP from phosphocreatine at discrete cellular sites of high ATP turnover (*36*, *37*). Neurofilament proteins (NF-L and NF-M) were also found at higher levels in the brains of the animals that ingested GSE—these are cytoskeletal components of neurons that are important in brain development as well as in neuronal maintenance (*38*).

Five proteins were significantly lower in amount in the brains of animals that ingested GSE —the ϵ isoform of 14-3-3 protein, GFAP, actin, vimentin, and polypeptides homologous with the polypeptide sequence predicted by the RIKEN cDNA (NM 025994); see also gi34872436. GFAP, actin, and vimentin are all cytoskeletal proteins in the brain that have been found in elevated amounts in AD (*20*) and in reactive glia (*39*). Beyond

Table 3. Protein Differences Induced by GSE Are in the Opposite Direction to Those in AD and in Mouse Models of Neurodegeneration[a]

protein name	AD[b]	GSK3-β[c]	Htau40-1[d]	GSE/CT
mitochondrial matrix protein precursor P60 (HSP-60)	–	–1.54, –2.11	ND[e]	+1.5
creatine kinase brain β chain	–	–2.16, –1.55	ND	+1.52 and new pI[f]
actin	ND	ND	ND	–1.62 and less complex[g]
GFAP	±	ND	ND	–1.61
14-3-3 ϵ	+	ND	ND	–1.6
α-enolase	+	+1.84	+1.94	less complex
γ-enolase	+	ND	+1.58	less complex
RIKEN cDNA (NM 025994)	ND	ND	ND	–1.56
HSC-70	–	ND	ND	+1.63
HSC-71	–	ND	ND	+1.91
neurofilament L triplet protein	–	–2.16, –2.36	–2.79	+1.63
neurofilament M triplet protein	ND	ND	ND	+1.73
vimentin	+	ND	ND	–1.52

[a] All of the proteins identified are significantly different in intensity or variability in this study; GSE/CT indicates the fold changes or nature of difference in isoform complexity in the GSE brain relative to the control brain. [b,c,d] These are the previous studies that identified proteomic differences between human AD and age-matched nondemented brain (*19*, *20*) and between transgenic mouse models of neurodegeneration and wild-type littermates (GSK3β, ref *21*); (Htau40-1, ref *22*). [e] Differences in these proteins were not detected in the study indicated. [f] For CK-BB, there was a shift of one of the spots to a different horizontal position in the gel or a new p*I*. [g] Certain spots underwent a reduction in complexity; these spots were always identified by MALDI-TOF MS and LC-ESI-MS/MS to be the same polypeptide as the spots at the original *x*,*y* locations. The proteomic study of the AD tissues did not have quantitative information, only the direction of the change, + or – (*19*).

its homology to swiprosin 1, which has a putative EF-hand calcium-binding domain (*40*), the rat protein homologous with RIKEN cDNA sequence NM 025994 remains to be discovered.

The statistical algorithm to detect differences in the variability of the protein spot intensities is described in full elsewhere (S. Meleth, J. Deshane, and H. Kim, unpublished observations). However, visual inspection of the proteins indicated by this method confirmed consistent differences in the pattern of isoforms/post-translational modifications for α- and γ-enolases, actin, and CK-BB such as in **Figures 4** and **5** (the latter two proteins were also shown to be different in amounts in the brains of the rats that ingested the GSE-supplemented diet). Enolase is the enzyme that converts 2-phosphoglycerate to phosphoenolpyruvate in the glycolytic pathway. The predominant dimers of this enzyme in the brain, $\alpha\gamma$ and $\gamma\gamma$, are neuron-specific, because the γ isoform is neuron-specific, whereas the $\alpha\alpha$ isoform is restricted to glial cells (*41*).

Previous proteomic studies in mammalian brain cataloged over 1700 proteins representing 437 genes from human fetal brain (*42*). Others examined the effects of aging (*43*), neurodegenerative disease (*44*), and expression of transgenes in models of AD (*21*, *22*). In old versus young rat brain, five protein spots were found to be down-regulated (corresponding to peroxiredoxin 2-like protein, stathmin, and apolipoprotein A1 precursor, as determined by MALDI-TOF MS) (*43*). Interestingly, peroxiredoxin 2 is up-regulated in several diseases associated with neurodegeneration such as Down syndrome, AD, and Pick's disease (*45*).

In the brains of transgenic mice expressing pathological levels of the longest isoform of human τ protein, 34 proteins differed in expression by at least 1.5-fold compared to wild-type mice (*22*). This study also identified in mutant (S9A) GSK-3β transgenic mice 51 differentially expressed proteins (*21*), some of which were identified in this study (see **Table 3**). Krapfenbauer et al. (*45*–*47*) also identified brain proteins (heat shock protein 27, glucose regulated protein 78, neurofilament proteins, α-internexin, tubulin α-1, dehydrolipoamide dehydrogenase, ATP synthase β chain, isocitrate dehydrogenase, and pyruvate kinase M1) that underwent changes in expression following intraperitoneal administration of the neurotoxin kainic acid.

Certain proteins have been suggested to be oxidized to higher extents in AD brain, namely, creatine kinase, glutamine synthase, ubiquitin carboxy-terminal hydrolase L-1, dihydropyrimidinase-related protein 2, α-enolase, and HSC-71 (*48*, *49*). It remains to be seen whether any of the modifications detected in the present study were oxidations, and if so, whether the GSE modulated these.

Several polyphenol-enriched dietary supplements prevented memory loss and cognitive impairment in animal behavior studies (*50*). *G. biloba* has recently been suggested to improve memory in a clinical trial (*51*), although this is controversial (*52*). Changes in amounts of certain mRNAs in the brain were reported in mice treated with *G. biloba* using DNA microarray analysis (*53*); a direct analysis of the protein changes, however, was not carried out. This report is thus the first to document multiple changes looking directly at protein expression in the brain, in response to a specific but complex dietary supplement. Given that GSE contains polyphenols, it was not unreasonable to hypothesize that ingestion of this dietary supplement would influence brain protein expression. What remains to be determined is whether the changes are due to the polyphenols and/or their metabolites acting directly in the brain or indirectly by modulating the metabolism of endogenous compounds in the gut during their enterohepatic circulation. Another possibility is regulation of signaling through the gut–brain axis via the nervous system. Finally, it remains to be seen how the protein changes demonstrated in this study are functionally related to neurodegeneration and memory loss. At this point, it can be stated that the changes described here in the proteins following ingestion of grape seed extract *were consistent with a neuroprotective action*, because the directions of the changes were opposite to those detected for the same proteins in diseased brains (see **Table 3**). Epidemiological data suggested that moderate consumption of red but not white wine was associated with a reduction in dementias, including AD (*54*), consistent with our hypothesis that the grape polyphenols enriched in red/purple grape skins and seeds are neuroprotective. The recent failure of traditional hormone replacement therapy to protect against postmenopausal cognitive impairment (*55*) alone provides urgent rationale for the development of products (perhaps based on the grape components such as used in this study) that will have neuroprotective actions in elderly women.

Because this study was a first experiment, looking at global changes in the brain, whole brain homogenate was examined;

future studies will examine selected brain regions such as the hippocampus or entorhinal cortex, regions that have been shown to be important in memory and cognitive function and that have been shown to be affected in AD. In view of the fact that dietary supplements enriched in polyphenols such as those in GSE are marketed for their "antioxidant activities," it will also be important to determine whether the proteins and the changes they underwent in response to GSE are "protected" when the animal or tissue is exposed experimentally to oxidative stress or inflammatory conditions. Although the data reported here indicate that ingestion of antioxidants affects specific proteins, some of which have been shown to be vulnerable to oxidation (*56*−*58*), the results also suggest that complex mixtures of polyphenols such as in GSE, and that one can expect from foods, have *complex* effects on mammalian tissues, including possible effects on gene expression as well as on protein modifications. Finally, it should be noted that the results in this study were obtained with normal young-adult rats, suggesting that ingestion of grape seed components and similar food-derived polyphenols may benefit the *non-aged* nondiseased brain. If follow-up experiments can define the bioactive polyphenols in GSE, gene transfer technology such as described by Xie et al. (*59*) will play an important role in "delivering" genetic pathways of interest in plants.

The goals of this study were twofold: first, to address our hypothesis that specific proteins were modulated in target tissues such as the brain by polyphenol-enriched preparations such as GSE, and, second, to analyze and describe the resulting data using rigorous proteomics and statistical methods. With the internet availability of genome and proteome databases, future nutrition studies will probe more and more the relationships between nutrients and genes and gene products, the proteins. This study illustrates how a multifaceted approach can quantitatively measure small, multiple changes in biological molecules caused by nutrients or non-nutrient food components such as the polyphenols. Continued studies such as this of specific proteins affected by food components will help to lay the foundation for understanding the role of nutrition in disease prevention and treatment.

ABBREVIATIONS USED

AD, Alzheimer's disease; CHAPS, 3-[(3-cholamidopropyl)-dimethylammonio]-1-propanesulfonate; CID, collision-induced dissociation; CK-BB, creatine kinase brain β chain; DA, discriminant analysis; EDTA, ethylenediaminetetraacetic acid; ESI, electrospray ionization; GFAP, glial fibrillary acidic protein; GSE, grape seed extract; GSK, glycogen synthase kinase; HSC, heat shock cognate protein; HSP, heat shock protein; IEF, isoelectric focusing; IPG, immobilized pH gradient; LC-MS/MS, liquid chromatography−tandem mass spectrometry; MALDI-TOF MS, matrix-assisted laser desorption ionization time-of-flight mass spectrometry; MOWSE, molecular weight search engine; NCBI, National Center for Bioinformatics; NF-L, neurofilament triplet protein light chain; NF-M, neurofilament triplet protein medium chain, PA, proanthocyanins; PCA, principal component analysis; PVDF, polyvinylidenedifluoride; SDA, stepwise discriminant analysis; SDS-PAGE, sodium dodecyl sulfate−polyacrylamide gel electrophoresis; TBP, tributylphosphine; TBST, Tris-buffered saline with 0.2% Tween-20.

ACKNOWLEDGMENT

The grape seed extract preparation used in this study was generously donated by Kikkoman Corporation (Chiba, Japan).

Supporting Information Available: Tables of grape seed extract composition and of all significantly different gel spots in GSE and control gels. This material is available free of charge via the Internet at http://pubs.acs.org.

LITERATURE CITED

(1) Fontanarosa, P. B.; Rennie, D.; DeAngelis, C. D. The need for regulation of dietary supplements—lessons from ephedra. *JAMA*−*J. Am. Med. Assoc.* **2003**, *289*, 1568−1570.

(2) Yamakoshi, J.; Kataoka, S.; Koga, T.; Ariga, T. Proanthocyanidin-rich extract from grape seeds attenuates the development of aortic atherosclerosis in cholesterol-fed rabbits. *Atherosclerosis* **1999**, *142*, 139−149.

(3) Pataki, T.; Bak, I.; Kovacs, P.; Bagchi, D.; Das, D. K.; Tosaki, A. Grape seed proanthocyanidins improved cardiac recovery during reperfusion after ischemia in isolated rat hearts. *Am. J. Clin. Nutr.* **2002**, *75*, 894−899.

(4) Bagchi, D.; Sen, C. K.; Ray, S. D.; Das, D. K.; Bagchi, M.; Preuss, H. G.; Vinson, J. A. Molecular mechanisms of cardioprotection by a novel grape seed proanthocyanidin extract. *Mutat. Res.* **2003**, *523*−*524*, 87−97.

(5) Bagchi, D.; Bagchi, M.; Stohs, S.; Ray, S. D.; Sen, C. K.; Preuss, H. G. Cellular protection with proanthocyanidins derived from grape seeds. *Ann. N. Y. Acad. Sci.* **2002**, *957*, 260−270.

(6) Joseph, J. A.; Shukitt-Hale, B.; Denisova, N. A.; Bielinski, D.; Martin, A.; McEwen, J. J.; Bickford, P. C. Reversals of age-related declines in neuronal signal transduction, cognitive, and motor behavioral deficits with blueberry, spinach, or strawberry dietary supplementation. *J. Neurosci.* **1999**, *19*, 8114−8121.

(7) Bastianetto, S.; Quirion, R. Natural extracts as possible protective agents of brain aging. *Cell. Mol. Biol.* **2002**, *48*, 693−697.

(8) Chandrasekaran, K.; Mehrabian, Z.; Spinnewyn, B.; Chinopoulos, C.; Drieu, K.; Fiskum, G. Bilobalide, a component of the *Ginkgo biloba* extract (EGb 761), protects against neuronal death in global brain ischemia and in glutamate-induced excitotoxicity. *Cell. Mol. Biol.* **2002**, *48*, 663−669.

(9) Kim, H.; Xia, H.; Li, L.; Gewin, J. Attenuation of neurodegeneration-relevant modifications of brain proteins by dietary soy. *Biofactors* **2000**, *12*, 243−250.

(10) Pan, Y.; Anthony, M.; Watson, S.; Clarkson, T. B. Soy phytoestrogens improve radial arm maze performance in ovariectomized retired breeder rats and do not attenuate benefits of 17β-estradiol treatment. *Menopause* **2000**, *7*, 230−235.

(11) Yamakoshi, J.; Saito, M.; Kataoka, S.; Kikuchi, M. Safety evaluation of proanthocyanidin-rich extract from grape seeds. *Food Chem. Toxicol.* **2002**, *40*, 599−607.

(12) Gibbons, J. D. In *Nonparametric Methods of Quantitative Analysis*; American Science Press: Columbus, OH, 1997; Chapter 4, pp 169−212.

(13) Mardia, K. V.; Kent, J. T.; Bibby, J. M. In *Multivariate Analysis*; TJ Press (Padstow): Cornwall, U.K., 1995; Chapter 11, pp 301−324.

(14) Mardia, K. V.; Kent, J. T.; Bibby, J. M. In *Multivariate Analysis*; TJ Press (Padstow): Cornwall, U.K., 1995; Chapter 8, pp 213−246.

(15) Tuma, R.; Coward, L. U.; Kirk, M. C.; Barnes, S.; Prevelige, P. E., Jr. Hydrogen−deuterium exchange as a probe of folding and assembly in viral capsids. *J. Mol. Biol.* **2001**, *23*, 389−396.

(16) Pappin, D. J. C.; Hojrup, P.; Bleasby, A. J. Rapid identification of proteins by peptide-mass fingerprinting. *Protein Sci.* **1993**, *3*, 327−332.

(17) Bleasby, A. J.; Wootton, J. C. Construction of validated, non-redundant composite protein sequence databases. *Protein Eng.* **1990**, *3*, 153−159.

(18) Carninci, P.; Hayashizaki, Y. High-efficiency full-length cDNA cloning. *Methods Enzymol.* **1999**, *303*, 19−44.

(19) Schonberger, S. J.; Edgar, P. F.; Kydd, R.; Faull, R. L. M.; Cooper, G. J. S. Proteomic analysis of the brain in Alzheimer's disease: Molecular phenotype of a complex disease process. *Proteomics* **2001**, *1*, 1519−1528.

(20) Tsuji, T.; Shiozaki, A.; Kohno, R.; Yoshizato, K.; Shimohama, S. Proteomic profiling and neurodegeneration in Alzheimer's disease. *Neurochem. Res.* **2002**, *27*, 1245−1253.

(21) Tilleman, K.; Stevens, I.; Spittaels, K.; Haute, C. V.; Clerens, S.; Van Den Bergh, G.; Geerts, H.; Van Leuven, F.; Vandesande, F.; Moens, L. Differential expression of brain proteins in glycogen synthase kinase-3 transgenic mice: a proteomics point of view. *Proteomics* **2002**, *2*, 94−104.

(22) Tilleman, K.; Van den Haute, C.; Geerts, H.; van Leuven, F.; Esmans, E. L.; Moens, L. Proteomics analysis of the neurodegeneration in the brain of tau transgenic mice. *Proteomics* **2002**, *2*, 656−665.

(23) Spittaels, K.; Van den Haute, C.; Van Dorpe, J.; Geerts, H.; Mercken, M.; Bruynseels, K.; Lasrado, R.; Vandezande, K.; Laenen, I.; Boon, T.; Van Lint, J.; Vandenheede, J.; Moechars, D.; Loos, R.; Van Leuven, F. Glycogen synthase kinase-3β phosphorylates protein tau and rescues the axonopathy in the central nervous system of human four-repeat tau transgenic mice. *J. Biol. Chem.* **2000**, *275*, 41340−41349.

(24) Spittaels, K.; Van den Haute, C.; Van Dorpe, J.; Bruynseels, K.; Vandezande, K.; Laenen, I.; Geerts, H.; Mercken, M.; Sciot, R.; Van Lommel, A.; Loos, R.; Van Leuven, F. Prominent axonopathy in the brain and spinal cord of transgenic mice overexpressing four-repeat human tau protein. *Am. J. Pathol.* **1999**, *155*, 2153−2165.

(25) Hirschi, K. D.; Kreps, J. A.; Hirschi, K. K. Molecular approaches to studying nutrient metabolism and function: an array of possibilities. *J. Nutr.* **2001**, *131*, 1605S−1609S.

(26) Muller, M.; Kersten, S. Nutrigenomics: goals and strategies. *Nat. Rev. Genet.* **2003**, *4*, 315−322.

(27) Ideker, T.; Thorsson, V.; Ranish, J. A.; Christmas, R.; Buhler, J.; Eng, J. K.; Bumgarner, R.; Goodlett, D. R.; Aebersold, R.; Hood, L. Integrated genomic and proteomic analyses of a systematically perturbed metabolic network. *Science* **2001**, *292*, 929−934.

(28) Washburn, M. P.; Ulaszek, R.; Deciu, C.; Schieltz, D. M.; Yates, J. R., 3rd. Analysis of quantitative proteomic data generated via multidimensional protein identification technology. *Anal. Chem.* **2002**, *74*, 1650−1657.

(29) Xiong, M.; Jin, L.; Li, W.; Boerwinkle, E. Computational methods for gene expression-based tumor classification. *Biotechniques* **2000**, *29*, 1264−1268.

(30) Mendez, M. A.; Hodar, C.; Vulpe, C.; Gonzalez, M.; Cambiazo, V. Discriminant analysis to evaluate clustering of gene expression data. *FEBS Lett.* **2002**, *522*, 24−28.

(31) Liu, A.; Zhang, Y.; Gehan, E.; Clarke, R. Block principal component analysis with application to gene microarray data classification. *Statist. Med.* **2002**, *21*, 3465−3474.

(32) Quackenbush, J. Microarray data normalization and transformation. *Nat. Genet.* **2002**, *32*, 496−501.

(33) Wise, M. J.; Littlejohn, T. G.; Humphery-Smith, I. Peptide-mass fingerprinting and the ideal covering set for protein characterization. *Electrophoresis* **1997**, *18*, 1399−1409.

(34) Reddy, R. K.; Lu, J.; Lee, A. S. The endoplasmic reticulum chaperone glycoprotein GRP94 with Ca^{2+}-binding and antiapoptotic properties is a novel proteolytic target of calpain during etoposide-induced apoptosis. *J. Biol. Chem.* **1999**, *274*, 28476−28483.

(35) Mosser, D. D.; Caron, A. W.; Bourget, L.; Meriin, A. B.; Sherman, M. Y.; Morimoto, R. I.; Massie, B. The chaperone function of hsp70 is required for protection against stress-induced apoptosis. *Mol. Cell. Biol.* **2000**, *20*, 7146−7159.

(36) Friedman, D. L.; Roberts, R. Compartment of brain-type creatine kinase and ubiquitous mitochondrial creatine kinase in neurons: evidence for a creatine phosphate energy shuttle in adult rat brain. *J. Comput. Neurol.* **1994**, *343*, 500−511.

(37) Wallimann, T.; Wyss, M.; Brdiczka, D.; Nicolay, K.; Eppenberger, H. M. Intracellular compartmentation, structure and function of creatine kinase isoenzymes in tissues with high and fluctuating energy demands: the 'phosphocreatine circuit' for cellular energy homeostasis. *Biochem. J.* **1992**, *281*, 21−40.

(38) Bajo, M.; Yoo, B. C.; Cairns, N.; Gratzer, M.; Lubec, G. Neurofilament proteins NF-L, NF-M and NF-H in brain of patients with Down syndrome and Alzheimer's disease. *Amino Acids* **2001**, *21*, 293−301.

(39) Oblinger, M. M.; Singh, L. D. Reactive astrocytes in neonate brain upregulate intermediate filament gene expression in response to axonal injury. *Int. J. Dev. Neurosci.* **1993**, *11*, 149−156.

(40) Kawai, J., et al. Functional annotation of a full-length mouse cDNA collection. *Nature* **2001**, *409*, 685−690.

(41) Messier, C.; Gagnon, M. Glucose regulation and cognitive functions: relation to Alzheimer's disease and diabetes. *Behav. Brain Res.* **1996**, *75*, 1−11.

(42) Fountoulakis, M.; Juranville, J. F.; Dierssen, M.; Lubec, G. Proteomic analysis of the fetal brain. *Proteomics* **2002**, *2*, 1547−1576.

(43) Chen, W.; Ji, J.; Xu, X.; He, S.; Ru, B.Proteomic comparison between human young and old brains by two-dimensional gel electrophoresis and identification of proteins. *Int. J. Dev. Neurosci.* **2003**, *21*, 209−216.

(44) Cheon, M. S.; Fountoulakis, M.; Dierssen, M.; Ferreres, J. C.; Lubec, G. Expression profiles of proteins in fetal brain with Down syndrome. *J. Neural Transmission, Suppl.* **2001**, *61*, 311−319.

(45) Krapfenbauer, K.; Engidawork, E.; Cairns, N.; Fountoulakis, M.; Lubec, G. Aberrant expression of peroxiredoxin subtypes in neurodegenerative disorders. *Brain Res.* **2003**, *967*, 152−160.

(46) Krapfenbauer, K.; Berger, M.; Lubec, G.; Fountoulakis, M. Changes in the brain protein levels following administration of kainic acid. *Electrophoresis* **2001**, *22*, 2086−2091.

(47) Krapfenbauer, K.; Berger, M.; Friedlein, A.; Lubec, G.; Fountoulakis, M. Changes in the levels of low-abundance brain proteins induced by kainic acid. *Eur. J. Biochem.* **2001**, *268*, 3532−3537.

(48) Korolainen, M. A.; Goldsteins, G.; Alafuzoff, I.; Koistinaho, J.; Pirttila, T. Proteomic analysis of protein oxidation in Alzheimer's disease brain. *Electrophoresis* **2002**, *23*, 3428−3433.

(49) Castegna, A.; Aksenov, M.; Thongboonkerd, V.; Klein, J. B.; Pierce, W. M.; Booze, R.; Markesbery, W. R.; Butterfield, D. A. Proteomic identification of oxidatively modified proteins in Alzheimer's disease brain. Part II: dihydropyrimidinase-related protein 2, α-enolase and heat shock cognate 71. *J. Neurochem.* **2002**, *82*, 1524−1532.

(50) Stackman, R. W.; Eckenstein, F.; Frei, B.; Kulhanek, D.; Nowlin, J.; Quinn, J. F. Prevention of age-related spatial memorydeficits in a transgenic mouse model of Alzheimer's disease by chronic *Ginkgo biloba* treatment. *Exp. Neurol.* **2003**, *184*, 510−520.

(51) Ercoli, L.; Small, G. W.; Silverman, D. H. S.; Sidarth, P.; Dorsey, D.; Miller, K.; Kaplan, A.; Skura, S.; Byrd, G.; Huang, S. C.; Phelps, M. E. The effects of *Ginkgo biloba* on cognitive and cerebral metabolic function in age-associated memory impairment. Presented at the 34th Annual Meeting of the Society for Neuroscience, 2003.

(52) van Dongen, M.; van Rossum, E.; Kessels, A.; Sielhorst, H.; Knipschild, P. Ginkgo for elderly people with dementia and age-associated memory impairment: a randomized clinical trial. *J. Clin. Epidemiol.* **2003**, *56*, 367−376.

(53) Watanabe, C. M.; Wolffram, S.; Ader, P.; Rimbach, G.; Packer, L.; Maguire, J. J.; Schultz, P. G.; Gohil, K. The in vivo neuromodulatory effects of the herbal medicine *Ginkgo biloba*. *Proc. Natl. Acad. Sci. U.S.A.* **2001**, *98*, 6577−6580.

(54) Truelsen, T.; Thudium, D.; Gronbaek, M. Amount and type of alcohol and risk of dementia: the Copenhagen City Heart Study. *Neurology* **2002**, *59*, 1313−1319.

(55) Shumaker, S. A.; Legault, C.; Rapp, S. R.; Thal, L.; Wallace, R. B.; Ockene, J. K.; Hendrix, S. L.; Jones, B. N., 3rd; Assaf, A. R.; Jackson, R. D.; Kotchen, J. M.; Wassertheil-Smoller, S.; Wactawski-Wende, J.; WHIMS Investigators. Estrogen plus progestin and the incidence of dementia and mild cognitive impairment in postmenopausal women: the Women's Health Initiative Memory Study: a randomized controlled trial. *JAMA—J. Am. Med. Assoc.* **2003**, *289*, 2651−2662.

(56) Aksenova, M. V.; Aksenov, M. Y.; Payne, R. M.; Trojanowski, J. Q.; Schmidt, M. L.; Carney, J. M.; Butterfield, D. A.; Markesbery, W. R. Oxidation of cytosolic proteins and expression of creatine kinase BB in frontal lobe in different neurodegenerative disorders. *Dement. Geriatr. Cogn. Disord.* **1999**, *10*, 158−165.

(57) Aksenov, M.; Aksenova, M.; Butterfield, D. A.; Markesbery, W. R. Oxidative modification of creatine kinase BB in Alzheimer's disease brain. *J. Neurochem.* **2000**, *74*, 2520−2527.

(58) Aksenov, M. Y.; Aksenova, M. V.; Butterfield, D. A.; Geddes, J. W.; Markesbery, W. R. Protein oxidation in the brain in Alzheimer's disease. *Neuroscience* **2001**, *103*, 373−383.

(59) Xie, D. Y.; Sharma, S. B.; Paiva, N. L.; Ferreira, D.; Dixon, R. A. Role of anthocyanidin reductase, encoded by BANYULS in plant flavonoid biosynthesis. *Science* **2003**, *299*, 396−399.

(60) Kim, H.; Hall, P.; Smith, M.; Kirk, M.; Prasin, J. K.; Barnes, S.; Grubbs, C. Chemoprevention by grape seed extract and genistein in carcinogen-induced mammary cancer in rats is diet dependent. *J. Nutr.* **2004**, *134*, 3445S−3452S.

Received for review September 28, 2004. Accepted November 12, 2004. This research was supported by a subcontract to H.K. from Purdue University (NIH/NCCAM P50 AT00477) as part of the Purdue−UAB Botanicals Center for Age-Related Diseases and by Grant DAMD17-01-1-0469 to H.K. from the U.S. Army Medical Research and Materiel Command. The mass spectrometers were purchased with NCRR Shared Instrumentation Grants S10RR11329 and S10RR13795 to S.B. and an award from the UAB Health Services Foundation General Endowment Fund. Ongoing support for mass spectrometry is provided by NCI Grant P30 CA-13148 to the UAB Comprehensive Cancer Center (A. LoBuglio, P.I.). The 2D Proteomics Laboratory has been supported by UAB Health Services Foundation General Endowment Fund awards to H.K. Specific proteomics instrumentation was purchased with NCRR Shared Instrumentation Grant S10-RR16849-01 to H.K.

JF040407D